Available online at www.sciencedirect.com
SCIENCE DIRECT
Cement and Concrete Research 35 (2005) 1555–1565
Cement and Concrete Research

Lime pozzolana mortars in Roman catacombs: composition, structures and restoration

Sergio Sánchez-Moral[a,*], Luis Luque[a], Juan-Carlos Cañaveras[b], Vicente Soler[c], Javier Garcia-Guinea[a], Alfredo Aparicio[a]

[a]Museo Nacional de Ciencias Naturales (CSIC), C/ José Gutiérrez Abascal 2, E-28006 Madrid, Spain
[b]Universidad de Alicante, Departamento de Ciencias Tierra and Medio Ambiente, E-03080 Alicante, Spain
[c]Instituto de Productos Naturales y Agrobiologia de Canarias, Avda, Astrofisico Francisco Sanchez 3, E-38206 La Laguna, Tenerife, Spain

Received 21 April 2003; accepted 19 August 2004

Abstract

Analyses of microsamples collected from Roman catacombs and samples of lime–pozzolana mortars hardened in the laboratory display higher contents in carbonated binder than other subaerial Roman monuments. The measured environmental data inside the Saint Callistus and Domitilla catacombs show a constant temperature of 15–17 °C, a high CO_2 content (1700 to 3500 ppm) and a relative humidity close to 100%. These conditions and particularly the high CO_2 concentration speed-up the lime calcitization roughly by 500% and reduce the cationic diffusion to form hydrous calcium aluminosilicates. The structure of Roman catacomb mortars shows (i) coarser aggregates and thicker beds on the inside, (ii) thin, smoothed, light and fine-grained external surfaces with low content of aggregates and (iii) paintings and frescoes on the outside. The observed high porosity of the mortars can be attributed to cracking after drying linked with the high binder content. Hardened lime lumps inside the binder denote low water/mortar ratios for slaking. The aggregate tephra pyroclasts rich in aluminosilicate phases with accessorial amounts of Ba, Sr, Rb, Cu and Pb were analysed through X-ray diffraction (XRD), electron microprobe analysis (EMPA) and also by environmental scanning electron microscopy (ESEM) to identify the size and distribution of porosity. Results support procedures using local materials, special mortars and classic techniques for restoration purposes in hypogeal backgrounds.

Keywords: $CaCO_3$; $Ca(OH)_2$; Mortar; Aggregate; Pozzolan; Microcracking; Crystal size; Curing

1. Introduction

Lime–pozzolana mortars cover large surfaces of Roman catacomb walls and are usually painted with frescoes (Fig. 1a). In the eastern part of Rome, outside the ancient walls, Saint Callistus and Domitilla are two of the oldest catacombs excavated in volcanic tuff. Saint Callistus is famous for the popes' tombs of the second century AD. These important archaeological–architectural heritages attract thousands of tourists. Many wall surfaces of Saint Callistus and Domitilla catacombs are made of volcanic rock dated to the middle Pleistocene originating from the Colli Albani volcanic district. Corridors are often partially covered with bricks making up the structural arches, walls and domes. Many cubicles containing family or communal tombs were dug as squared dome shapes and covered with mortar and stuccoes (Fig. 1b). Mortar prevents failure of the soft substrate and provides a clean, plain, light surface to be decorated with religious paintings and symbols. The catacombs were built from the second to the eighth century AD, and the main part of the decorated mortar originates from the first stages of the catacomb use.

The excellent properties of lime–pozzolana mortars, such as high strength, insolubility and hardening even under water, were known to the ancient Roman builders since the third century BC. Significant Roman monuments, such as

* Corresponding author.
E-mail address: ssmilk@mncn.csic.es (S. Sánchez-Moral).

0008-8846/$ - see front matter © 2004 Elsevier Ltd. All rights reserved.
doi:10.1016/j.cemconres.2004.08.009

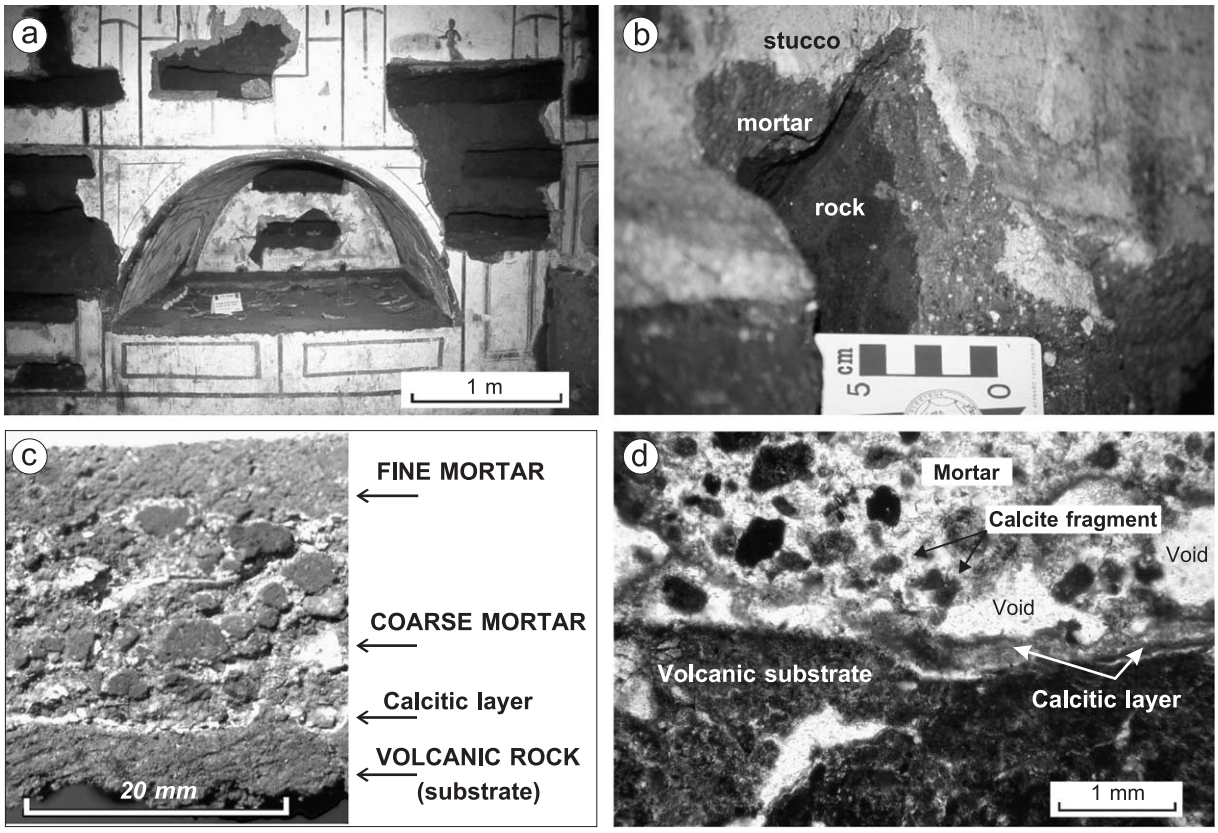

Fig. 1. (a) Aspect of walls in a cubicle covered by mortar and painted frescoes in the Saint Callistus catacomb (Rome). (b) Section showing the volcanic substrate overlaid by thin layers of mortar and stucco. (c) Section of individual sample showing coarse and fine aggregate inside the mortar beds and pure calcite in the mortar substrate interface. (d) Thin section of both the volcanic substrate and the mortar with two thin calcite layers overcoating the substrate.

the Pantheon, Roman Baths or Coliseum in Rome, were built using Roman concrete called "Opus Caementicium" in the first century AD [1]. The structural and physical–chemical characterization of the lime–pozzolana mortars used in building and the determination of the prevailing microenvironmental conditions could provide enough information to formulate new specific mortars for restoration purposes, using original neighbouring raw materials. The region of Rome is volcanic in nature, and the hills of the City consist of a relatively soft and light volcanic material known as tuff. In different places, it has slightly different textures and colours (grey, brown, and black are typical), but it is always lighter than lava, very coarse-grained with numerous small cavities. Unfortunately, recent restorations using inadequate materials incompatible with the original bedding mortar may cause permanent damage [2]. The use of physically–chemically suitable mortar, aesthetically compatible, must help restoration works [2–5]. Detailed studies on historical mortars sampled in the Roman catacombs may contribute to understanding the aspects of missing traditional techniques.

The aim of this work is to determine the chemical and mineralogical composition, texture, structure and properties of lime–pozzolana mortars from Roman catacombs. The research concentrated on three aspects of research: (i) studying microsamples collected from the wall catacombs by optical microscopy, environmental scanning electron microscopy (ESEM), electron microprobe (EM), X-ray diffraction (XRD), ICP-AES, atomic absorption spectroscopy (AAS), porosimetry, etc.; (ii) performing original experiments of lime–pozzolana hardening under X-ray diffraction with thermal control; and (iii) measuring the environmental data inside catacombs (RH values, CO_2 concentration, temperature, pH and chemical composition of infiltration waters).

2. Method and techniques

2.1. Environmental data

Microclimatic parameters were measured by installing a monitoring system consisting of microsensor instruments, a PC-based data logger system and a signal-conditioning unit inside Saint Callistus catacomb. Microsensors installed on air/floor/lamps measured temperature (measurement accuracy 0.01 °C), air relative humidity (0.1%), air CO_2 concentration (2.8 ppm) and ^{222}Rn concentration (pylon AB5 scintillometer with a diffusion detector). Automatic recording of data every 2 min was performed during 6

months. This information will be helpful in understanding the mortar hardening and preservation conditions. Also, an external weather station was installed outside the catacomb to record outdoor conditions.

2.2. Samples and microscopy

To reduce damage in the ancient walls, mortar samples ranging from 5 to 30 g were carefully collected from Saint Callistus and Domitilla catacombs, using a scalpel, a small chisel and a little hammer. Samples were observed under the stereomicroscope to separate different layers for subsequent analysis. Optical observation of small chips of the samples cut-polished in thin sections up to 35 μm in thickness was done, using a polarizing microscope (Nikon Eclipse C600 POL) equipped with a digital Nikon Coolpix 950 camera. In this manner, the mineralogy and type of aggregate, binder, porosity, cracking, secondary mineral formation and binder–aggregate ratios were determined. Morphology, textures, relationships, composition, crystal shapes and sizes of lime–pozzolana mortars were also studied by environmental scanning electron microscopy (ESEM). For this technique, sample metallisation was done using gold vapour in vacuum (50 Å of gold cover) in a Bio-Rad SC515 sputter coating unit. Samples were observed in a Philips XL20 SEM at accelerating voltages of 20–30 kV. The EDS analyses were obtained using a Phillips EDAX PV9900 with a light element detector type ECON. The porosity was determined by two methods, microscopy of thin sections and mercury intrusion porosimetry, using a Micromeritics Autopore III S 9400.

2.3. Chemical and structural analyses

The chemical and mineralogical composition of individual mineral grains was determined by electron microprobe (EM; Jeol Superprobe JXA-8900M), bulk and channel-selected (TAP, PETJ, LIF, PETH) X-ray spectra search and identification routines. The standards used were natural and synthetic crystals from the collection of the "Servicio de Microscopía Electrónica Lluis Bru," Complutense University, Madrid. The chemical composition of mortar components was obtained through several techniques such as inductively coupled plasma-mass spectrometry (ICP-MS) for trace elements; atomic absorption spectroscopy (AAS) and electron microprobe analysis (EMPA) for major and minor elements. The concentration of ferrous iron was determined by wet chemistry using a redox titration with ceric sulphate as titrant, measured with an ORP electrode. The semiquantitative mineral composition of the lime–pozzolana mortars was determined through X-ray diffraction (XRD) using a Phillips PW-1710 powder diffractometer with CuKα radiation. Patterns were obtained by step scanning from 3° to 75° 2θ with a count of 0.2 s per step, exploration speed of 2°/min at 40 kV and 40 mA.

2.4. Experimental reaction by a self-isothermal XRD

The experimental in situ hardening of different mixtures of portlandite–pozzolana mortars was performed in a self-made chamber for X-ray diffraction during which a sequential test was performed for 132 h. The procedure was as follows: (1) a continuous experiment for 13 h, recording first 265 isothermal XRD sequential profiles of 3 min each at 17 °C from 27° to 38° 2θ; (2) six subsequent series of 24 XRD profiles each, approximately for 1 h at 17°C, after addition of water to the sample to observe portlandite carbonation under completely wet conditions; and (3) additional series of 24 XRD profiles in the same wet conditions after 1 day and 1 weekend to evaluate the progress of the carbonation. These XRD profiles, recorded under thermally controlled conditions, were performed using a Phillips PW1710/00 powder diffractometer with CuKα radiation. Patterns were obtained by step scanning from 27° to 38° 2θ in 0.05 steps with a count of 2 s per step. Improvements made to the X-ray diffractometer include (a) a new original water refrigerator; (b) a new stainless steel door to hold internal cooling fluids; (c) internal heaters (resistance and halogen lamp) in new sample holders under PID thermal control; (d) a new electronic circuit and software to record differential thermal analyses between the sample and reference; and (e) a specific subdoor to fit the relative humidity detector [6,7]. The simplest method was to modify only the door of the sample chamber; a new rounded door was constructed to fit newly constructed and marketable supplies. A self-made MS-DOS program package, i.e., PLV-SIRDAT by J. D. Martin-Ramos (jdmartin@goliat.ugr.es), was used for the full-duplex control of the X-ray diffractometer (Philips PW1710/00 with a PW1712 communication card) via a RS232 serial port. PLV is made up of several programs: (a) REGISTRO—to control and acquire diffraction data; (b) LECTOR—a diffractogram evaluation program; (c) X—a program for fully automatic phase identification in mixtures with sine and cosine 2θ corrections; and (d) R—for refining cell parameters. SIRDAT is a specific program that allows sequential data records to be processed.

3. Results

3.1. Environment data

Microenvironmental recordings inside the catacombs show humidity values close to saturation (relative humidity ≥97%), high CO_2 concentrations (1700 and 3500 ppm in the Domitilla and Saint Callistus catacombs) and a constant temperature of 15–17 °C during most of the year. Infiltration waters are scarce. Only two dripping points could be sampled in the Saint Callistus catacomb. Water chemistry shows pH values (7.5 and 7.8) close to neutral and locally high concentrations of nitrates (148 ppm), which could be

explained by the farming activity in the surrounding landscape. Minor values of sulphate (46 and 33 ppm) have also been observed. CO_2 partial pressure was $10^{-2.06}$ to $10^{-1.97}$ bar. The microclimate monitoring system measuring temperature, relative humidity and CO_2 concentration was operative in Domitilla and Saint Callistus catacombs.

Recently, lighting time, air and rock temperature and ^{222}Rn concentration are being measured in the Saint Callistus catacomb. A new sensor detecting temperature differences between the air and rock surface was also installed in the Oceanus cubiculum. This wealth of new data will be used in additional studies regarding the impact of tourists visiting the architectural heritage.

3.2. Mortar characterization

Mortar-coating thickness onto the volcanic substrate ranges from 2 to 20 mm. Mortars are composed of one, two or three separate beds with different sizes and shapes of aggregates (Fig. 1c). Usually, the mortar shows only two layers: the inner ranging from 11 to 13 mm and the outer from 0.3 to 0.6 mm. The external surface of mortars often displays areas with a smooth grey–white–brown colour. A mixture of volcanic rock aggregate and calcite binder forms the common Roman mortar from catacombs. Mortar beds coating the rock surface or covering former mortars are thicker and comprise coarser aggregates. External beds are usually composed of fine volcanic dust and calcite. One analysed mortar sample shows a thin layer of quartz fragments mixed with lime, covering the volcanic aggregate mortar. Frequently, the rock-mortar interface shows a thin bed of pure calcite binding both surfaces (Fig. 1c, d). The lime mortar displays two or three separated beds including occasional air pockets among them. Thin sections of aggregate tuffs show calcite in the fissures. Under the polarizing microscope, thin sections of mortars show aggregate/binder ratios ranging from 0.5:1 to 1.1:1 (Fig. 1d), being highly variable even inside a single sample. Aggregate grain sizes are also highly variable. It is possible to distinguish two sizes of population in the coarse mortars, one from 0.5 to 2 mm and one from 100 to 300 μm. The grain size distribution is apparently bimodal. Mortar aggregates are composed of small fragments of tephra (Fig. 1d), which is a frequent substrate volcanic rock in the Lazio region, almost certainly obtained by digging galleries and tombs. These fragments show pyroxene phenocrysts (8–14% of augite–aegirine rich in Na and Fe), sanidine, biotite, analcime (20%), phyllosilicate phases and calcite (5–10%). Occasionally, they are mixed with detrital sandy quartz in a vitreous glassy matrix. This matrix could be the main component of the whole rock. The aggregate is composed of fragments of vitreous volcanic rock, usually including euhedral phenocrysts with sharp edges and irregular shapes. Different sources of pyroclastic rocks are assumed, given that phenocrysts are more abundant in the mortar aggregates than in the surrounding substrate. Likewise, X-ray diffraction analyses show divergence between the substrate pyroclasts and the aggregates composition (Table 1). Phyllosilicates are much more abundant in the host rock than in the aggregate, in respect to pyroxenes (3:1 in mortar versus 8:1 in host rock). Secondary minerals, such as analcime, are more abundant in the mortars than in the host rock. Occasionally, no feldspars occur in the mortar, but analcime and secondary products are detected. Possible secondary gypsum was observed in three samples in percentages less than 5%. Large calcite fragments are also found as aggregate (Fig. 1d). Lime masses remaining isolated after the slaking can explain them. Both the mortar aggregates and the volcanic rocks are rich in iron aluminosilicate phases (approximately 50%; Table 2). The CaO content is also important, mainly in mortar samples (ca. 17%). The initial ratios of ferrous versus ferric iron in the pyroclastic rocks point to the redox conditions of crystallization (e.g., 1:4.9 for the analysed samples of substrate). In addition, this (Fe^{2+}/Fe^{3+}) ratio is a sensitive indicator of the oxidation state (e.g., 1:2.5 in the mortar samples analysed). During weathering processes, Fe (III) is more conservative than Fe (II). The increment in the proportion of Fe (III) versus Fe (II) indicates more intense weathering of the rock [8,9] from its formation until its use. Roman builders would select the volcanic rock less altered for use as aggregate in the mortars. The trace element concentrations of mortars studied are quite homogeneous, and they are linked with the frequent addition of fresh tuff fragments. Barium and strontium are the most abundant trace elements in both rock and mortars. The most remarkable feature is the high content in copper, lead and rubidium of the mortars in comparison with the volcanic rocks. This could be related to the composition of the recipients in which the mortars were prepared. Mortars show high values of loss on ignition ranging from 17% to 25%, in connection with its high content in calcium carbonate. Mercury porosimetry measurements (Fig. 2) indicate that volcanic rock and mortar show a large porosity, averaging ca. 42%, while external mortar beds or stucco show a lower porosity, ca. 39%. The pore size distribution is homogeneous, all being below 100 μm (Fig. 2). Observations by ESEM and polarizing microscopy of

Table 1
Average mineral composition of volcanic rock (15 samples), coarse mortar (18 samples) and fine mortar (12 samples)

Material	Phyllosilicate	Augite	Feldspar	Quartz	Analcime	Calcite	Gypsum
Volcanic rock	68	10	5	<2	10	5	–
Coarse mortar	30	10	2	<3	14	42	1
Fine mortar	13	2	2	3	6	74	–

Table 2
Average bulk material elemental analyses—volcanic rock (15 samples), coarse mortar (18 samples) and fine mortar (12 samples)

Material	SiO_2	TiO_2	Al_2O_3	Fe_2O_3	FeO	MnO	MgO	CaO	Na_2O	K_2O	P_2O_5	LOI
Volcanic rock	45.28	0.68	18.55	6.88	1.21	0.22	2.22	7.16	2.18	2.09	0.27	13.04
Coarse mortar	35.32	0.43	12.31	3.73	1.45	0.15	1.95	19.39	1.95	1.25	0.29	21.44
Fine mortar	27.55	0.33	10.11	3.53	0.69	0.10	1.99	28.98	1.23	1.22	0.15	24.07

Material	Ba	Sr	Rb	Zr	Pb	Ce	La	U	Th	Li	V	Cu
Volcanic rock	2068	1101	266	363	119	255	149	10	67	61	191	46
Coarse mortar	1538	923	332	250	170	193	114	9	50	46	147	116
Fine mortar	2440	1183	334	256	269	201	117	9	50	45	150	68

Major oxides and loss on ignition (LOI) in wt.%, trace elements in ppm.

mortar thin sections (Fig. 3a) link this large porosity with the main fissures and orthogonal cracking. A network of fissures reaches up to the external surface, helping mineral dissolution. Fissures occur while the sample hardens by fast reduction during cooling in new atmospheric conditions. Occasionally, calcite masses fill these cracks (Fig. 3b).

3.3. Mortar hardening calculations

The mortar carbonation or hardening is a complex process that includes several consecutive reactions. The first step in the lime putty preparation is to dissolve the calcium hydroxide in water:

$$Ca(OH)_2 \leftrightarrow Ca^{2+} + (OH)_2^-$$

A saturated solution with pH 12.8 is produced. Before total slaked lime dissolution, carbonate ions come into the process, originating from atmospheric carbon dioxide. The rate of CO_2 uptake by water is relatively fast. The halftime of the reaction $CO_2(g)=CO_2(aq)$ is only minutes and decreases with increasing air CO_2 pressure [10]. The subsequent formation of carbonic acid is very fast (halftime

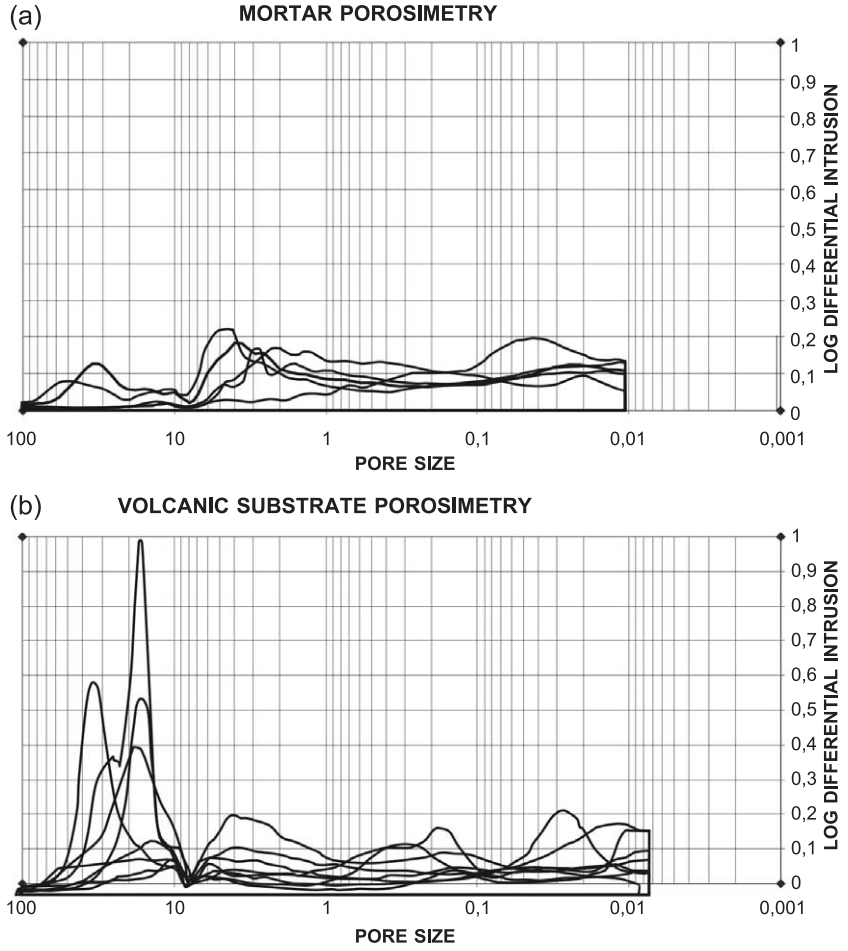

Fig. 2. Mercury porosimetry results of both samples: (a) mortar and (b) volcanic substrate. Note the large differences.

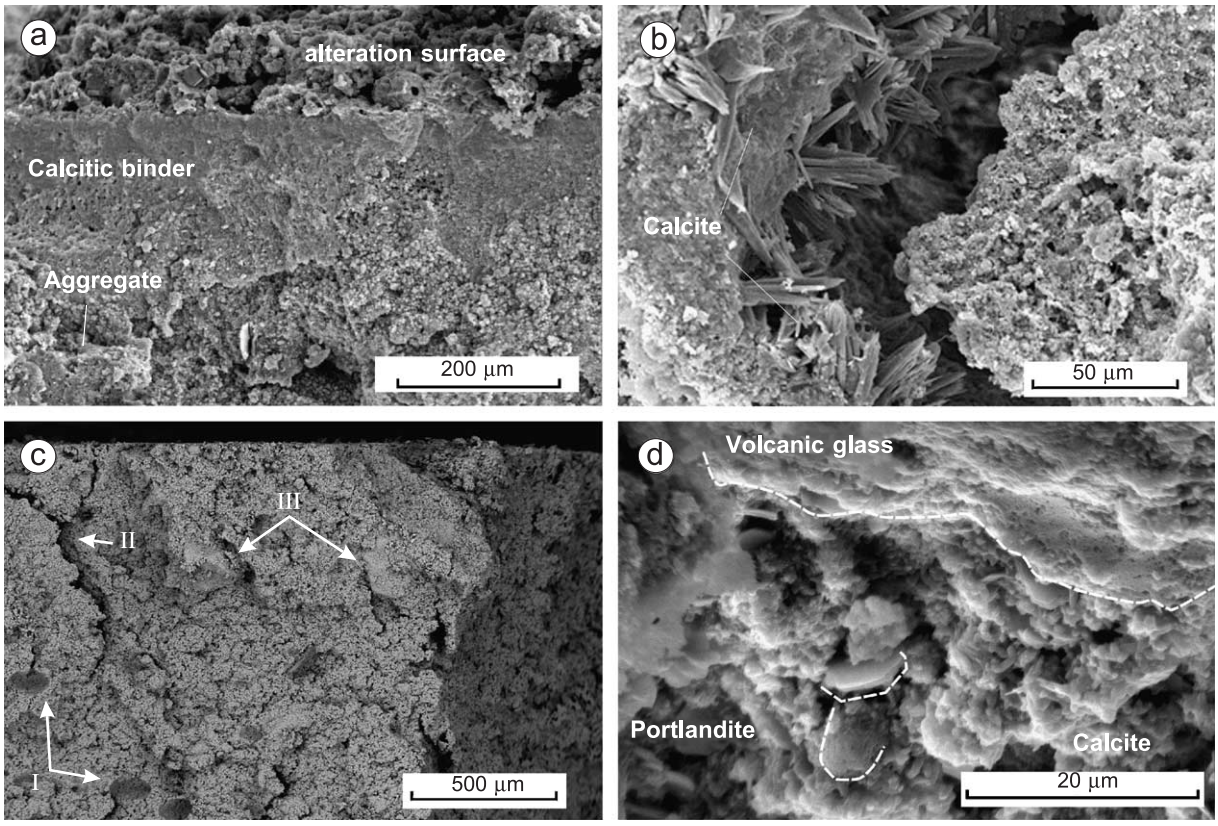

Fig. 3. ESEM photomicrographs of ancient Roman and experimental mortar samples: (a) layers of mortar and stucco and surface alterations; (b) orthogonal fissure filled by neoformed calcitic fibbers; (c) experimental mortar section showing: (I) voids left by loss of aggregates, (II) orthogonal cracks and fissures, (III) aggregate inside calcitic binder; (d) experimental mortar interface between volcanic aggregate and calcite binder showing remaining portlandite crystals.

~0.1 s), being close to 10^{-6} times the halftime of the homogeneous reaction:

$$H_2CO_3^0 \leftrightarrow H^+ + HCO_3^-$$

For this reason, the complete reaction–formation of calcium and carbonate species is fast enough to achieve equilibrium in few minutes. Calcite precipitation–dissolution is described by the overall reaction [11]:

$$Ca^{2+} + 2HCO_3^- \leftrightarrow CaCO_3(\text{calcite}) + CO_2(g) + H_2O$$

In which the essential reactions with their respective rate constants (k) are as follows:

$$Ca^{2+} + HCO_3^- \leftrightarrow CaCO_3 + H^+$$

with a rate constant k_1

$$Ca^{2+} + HCO_3^- \leftrightarrow CaCO_3 + H_2CO_3$$

with a rate constant k_2

$$Ca^{2+} + HCO_3^- + OH - \leftrightarrow CaCO_3 + H_2O$$

with a rate constant k_3.

Considering constant Pco_2 and temperature and assuming no inhibition for absorbed particles, the rate of solution or calcite precipitation is given by the sum of the rates of its elementary reactions and may be written as follows:

$$R = k_4[Ca^{2+}][HCO_3^-] - k_1[H^+] - k_2[H_2CO_2] - k_3[H_2O]$$

where R is in mmol/cm^2 s, and brackets denote activities. The value of k_4 is a function of temperature and Pco_2. For $Pco_2 < 10^{-1.5}$ bar, the function

$$\log k_4 = -7.56 + 0.016T - 0.64 \log Pco_2$$

(T in Kelvin, Pco_2 in bars) allows the rough calculation of the rate constant k_4 [10]. Temperature functions and rate constants have been suggested in previous publications [11,12].

Through this equation, using the PHRQPITZ software [13], the theoretical rate of calcite precipitation from a calcium hydroxide saturated solution under different air Pco_2 values and a constant temperature (15 °C) has been calculated. An open carbonate system was assumed where the CO_2 is continuously restocked by gaseous exchange. The value used for the equilibrium constant for calcite at 25 °C was ($-\log K_{eq}$=8.48; [14]). Two values have been chosen to simulate a hypothetical hardening process of lime putty: a Pco_2 of $10^{-3.7}$ bar that could correspond to the external atmosphere over the catacomb and $10^{-2.6}$ bar, a similar value to that measured inside by the microenvironmental monitoring.

Fig. 4 shows how the calcite precipitation rate increases together with the CO_2 partial pressure, although the total precipitated volume is slightly smaller for the highest CO_2 values. Calcite precipitation immediately begins when the

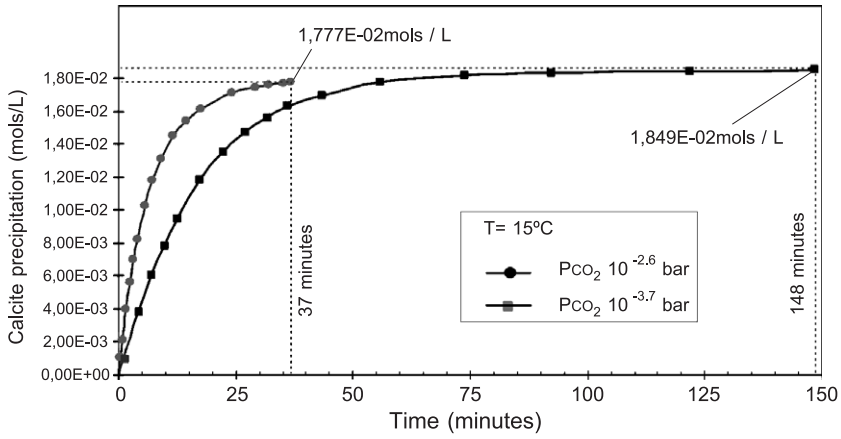

Fig. 4. Calcite precipitation rate under normal ($10^{-3.7}$ bar) and high ($10^{-2.6}$ bar) CO_2 pressure environment.

saturated solution is kept in touch with CO_2. This process could explain the observed large calcite fragments in the mortars. The initial high rates decrease very fast in respect to the calcite precipitation. In open-air environments, with Pco_2 values similar to hypogeal backgrounds, lime solution achieves saturation with respect to calcite in 37 min, four times quicker that in the case of atmospheric CO_2 pressures.

3.4. Mortar hardening measurements by XRD at 17 °C

Previous calculations allow a test on in situ hardening of Roman mortars composed of pure slaked lime and grinded volcanic aggregate from the catacombs. The result is a fine-grained mortar with microstructural features close to the original fine-grained Roman mortar (Fig. 3c). Observation by ESEM of the experimental mortars show fissures linked with sample hardening, which resembles those of the original mortars. The experimental mortars display a smaller cohesion between aggregates and binder (Figs. 3–6). This smaller cohesion could be associated with the incomplete carbonation demonstrated by the presence of small portlandite crystals in the innermost part of the experimental mortar (Fig. 3d).

The experiment was performed in a self-made chamber for X-ray diffraction, where 847 sequential XRD profiles of calcite and portlandite phases were recorded for 132 h. Measurements were limited to the angular region from 27° to 38° 2θ to observe the gradual growth of XRD peaks of calcite (3.03–2.84–2.49 Å) and the decrease of portlandite XRD peaks (3.11–2.63–2.44 Å), as shown in Fig. 5. In good agreement with the predicted portlandite–calcite phase transition, the main exchanges of peak sizes were observed during the first step of the test, in the initial 13 h. However, in the subsequent XRD profile series, after water addition, only slow changes are observed (Fig. 5b). The parameterisation of the XRD measurements was carried out analysing the full width, half maximum, using the PLV-SIRDAT software of Dr. Martin-Ramos, for the main XRD peaks of calcite and portlandite phases. The FWHM data were

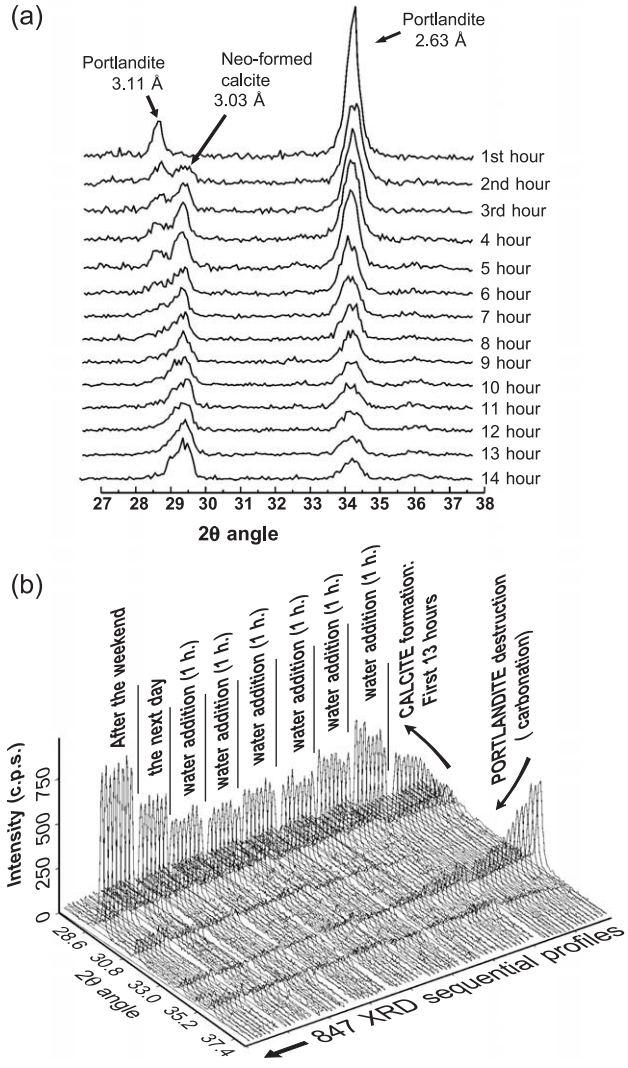

Fig. 5. Mineralogical evolution of experimental mortar in the XRD sequential profiles: (a) fast portlandite substitution by calcite in the first hours of hardening, (b) complete mineralogical evolution of mortar during experiment. Note the progressive and partial removal of portlandite linked with the calcite neoformation during the carbonation process.

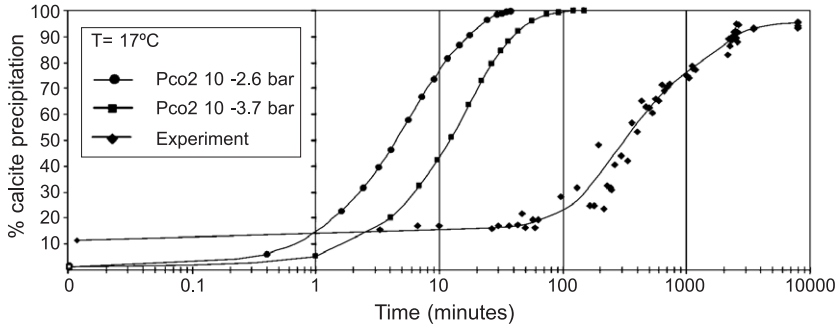

Fig. 6. Theoretical evolution of calcitization rate in different pCO_2 ($10^{-3.7}$ and $10^{-2.6}$ bar) conditions and real data obtained through XRD under standard conditions.

plotted versus time to be compared to theoretical calculations. Both results, experimental and theoretical hardening, display similar paths. The experimental carbonation of the portlandite phase, however, is slower than those forecasted by the calculations (Fig. 6).

4. Discussion

Traditional Roman mortar handling techniques nowadays are accepted to produce restoration lime mortar. [1,2,4,5]. Romans carried lime putty in baskets and mixed aggregate from local sources just before its application [15]. Lime–pozzolana mortar is a mixture of aggregate and lime. Lime (CaO) is produced by heating limestone ($CaCO_3$) to ca. 900 °C. The resultant quicklime (CaO) is mixed with water to obtain slaked lime ($Ca(OH)_2$). The final concrete results from the addition of surrounding aggregate materials, such as quartz sand, grog and rocks [1]. From the third century BC onwards, in the Lazio region, the use of volcanic rocks was widespread, thanks to their fast hardening, easy handling and high strength even under water and under fire. The characteristics and strength properties of a mortar arise from the composition of aggregate and binder and the specific evolution during hardening [16]; this last factor depends on placing techniques and environment.

4.1. Mortar volcanic aggregates

All aggregate components studied, with a few exceptions, are volcanic rocks. Mortar observation shows two or three stratified beds thinning outward. The use of several coating beds prevents the cracking of walls [1]. Aggregate sizes change depending on the bed depth, as has been observed in other Roman monuments [3]. The inner first layers are less aesthetic and display minor porosity as a result of mixed aggregates sizes. Mixed sizes of coarse aggregates with a slight amount of pozzolanic dust aggregate in the walls increase the reactive surface [17] and increase the calcitization speed [16]. The bimodal grain size distribution probably indicates a separate fragmentation of the volcanic rocks, first obtaining grains of ca. 1–2 mm and later producing a thin dust of volcanic aggregate, sized below 200 μm. External thinner bed and stuccoes provide a smooth surface to be decorated with frescoes. Unfortunately, these are often fissured by shrinking, as could be observed under the microscope. The volcanic aggregates contain a considerable amount of vitreous matrix and unstable minerals, such as sanidine feldspar, favouring chemical reactions with the lime in the interfaces. This reinforces the binding. The irregular fragments' shapes also increase the aggregate–binder reactive surface improving the bonding and decreasing the shrinking of the mortar, resulting in a higher cohesion and strength but a lower plasticity of the mixture [18,19]. Differences in mineralogical and chemical composition and alteration degree imply that the aggregates do not originate from around the catacombs at the same point of the final building. It is suggested that the high content in detritic and secondary clays (sometimes up to 80%) of the local material led the Roman builders to employ altered volcanic materials from different sources. The content in pozzolanic components, such as pyroxene, sanidine and volcanic glass, could be a reason for this. Vitruvius, in the first century, reported a preference for sands with low clay content [1]. While it is clear that Roman builders often used local materials, nevertheless, they selected well-known substances with the best behaviour.

4.2. Carbonated binder and environmental CO_2

Two factors help hardening during the mortar carbonation: (i) high CO_2 concentrations in the catacombs' environment and (ii) high porosity through fissures that allow an extra interchange surface assimilating carbon dioxide [19]. The high humidity and high CO_2 concentration in catacombs' microenvironment are favourable conditions for calcitization. [16]. Human breathing by builders, inhabitants or visitors produces extra CO_2. The low thickness of the mortar bed also helps a fast carbonation, inasmuch as surface hardening is fast, but at depth, hardening can take several years depending on environmental conditions, porosity and thickness [19]. Carbonation is a long-term process taking many months; extremely fast carbonation

could inhibit slower pozzolanic reactions, reducing the cationic diffusion.

The main difference between the theoretical kinetic mode and the experimental simulation carried out is the initial assumption of an open carbonate system in the former. The gradual calcification of the mortar causes a progressive closure of the system. Subsequently, the CO_2 in the mixture is not totally restocked, hindering sometimes a complete carbonation. Mortars, under real conditions, evolve in open, closed and mixed situations. The high porosity of the Roman mortars and the high CO_2 concentration inside the catacombs help CO_2 absorption by the mixture. However, carbonation is faster in a completely open system. The slow hardening of the flowing mixture produced by the fast carbonation in the high CO_2 environment of catacombs could have stimulated the Roman builders to increase the binder amount in respect to the aggregate. An important factor to be considered in the chemical reactions at the binder–aggregate boundaries is the pH inasmuch as a high pH more easily induces reactions of amorphous silicates, such as volcanic glass. During a common calcitization process, the pH decreases from 12.5 to 7–8 [16], and the aforementioned chemical reactivity is reduced.

The Pco_2 average values of the catacombs' environment lead to the lime solutions achieving saturation with respect to calcite in a short time (ca. 37 min), involving a very fast decrease in pH (Fig. 7), which could inhibit chemical reactions between aggregate and lime. Fast calcitization of the binder under higher concentrations of atmospheric CO_2 means a pH reduction and low reactivity of the mortars. For this reason, after CO_2 exposure, thin layers of lime mortar are formed. This differs from the classic pattern of pozzolanic mortars. The physical properties of mortars in the catacombs are supported more in the binder carbonation than in the pozzolanic activity. In this sense, it is important to stress that mortars in catacombs were not used as structural framework but for covering ceilings and walls

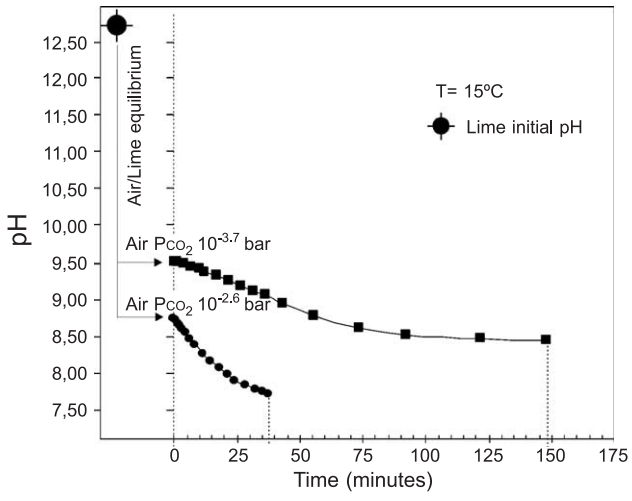

Fig. 7. Theoretical rate of the pH decrease during lime putty calcitization under different pCO_2 environmental conditions.

to avoid detachment of rock fragments and to decorate tombs and crypts.

The unexpectedly high porosity of the analysed mortars does not agree with the traditional water resistance and high strength of Roman mortars having smaller porosity. The microscopy study of the pore size distribution support as the porosity of volcanic fragments is very different to that of the mortar. The substrate porosity is mainly formed by intergranular spaces, while the mortar porosity is caused by parallel fissures produced by volume losses during a faster hardening of the surface. Larger pores are empirically linked to coarser grains and imply higher CO_2 diffusion and faster calcitization [16]. Calcite minerals have partially filled the pores; several dissolution–precipitation processes of calcium carbonate have also been noted in the fissures (Fig. 3b).

4.3. Ancient Roman technique to coat walls in hypogeal environments

Vitruvius explained, about pozzolanic mortars, that the convenient aggregate–lime ratio is 3:1 [1]. Plinius, in the first century AD, proposed a 4:1 ratio [20]. Different authors have observed similar ratios in ancient mortars of Roman monuments but usually with aggregate ratios closer to 2:1 [3,4]. Petrographical study of the Roman catacombs' mortars by polarised light microscope shows that the aggregate–binder ratio is highly variable, ranging from 0.5:1 to 1.1:1. This proportion shows larger quantities of lime but still far from those employed in the building of harbour infrastructures and breakwaters (2:1) [1] and those observed in other monuments [4,21]. The increase on the lime amount could be a useful technique for special environmental conditions, such as the catacombs, where calcitization is extremely fast. It could help setting onto vertical surfaces in high humidity. The mechanical consequence of mortars with high lime contents has higher strengths but also a higher risk of cracking through volume changes during hardening [19].

Limestone lumps inside mortar are linked with lime fragments not slaked due to water shortage during the slaking process. Most of the observed micritic fragments in the catacomb walls are slightly rounded or as pyramidal shapes formed in the mixture, hardened on the surface and were later included, still soft, in the remaining binder. This could be in good agreement with dry-slaking techniques using low water–binder ratios [2,16]. Low water–lime ratios mean low diffusion rate, and secondary formation in the interfacial transition zone is denser [22]. In some cases, radial crystal growth around voids indicates a secondary origin after volcanic glass dissolution. The pronounced mechanical and chemical differences between lime and volcanic rock may cause wall flaking in many areas of the catacombs. Voids and small discontinuities between beds suggest that builders waited for the first layer to set before placing the second layer and the following coarse mortar.

The calcitization rate of pure lime depends on the atmospheric CO_2 content. Using the chemical composition and the stoichiometric reactions proposed by Plummer et al. [23], it is observed that wet lime under 3000 ppm CO_2 calcitizes five times faster than in normal conditions (standard 270 ppm; Fig. 6). This example is applied to an open system assuming a thin layer in touch with air. In the case of thicker layers, the calcitization rate decreases inasmuch as the total bed changes to an almost closed system as a consequence of the external fast calcitization that blocks the contact with the atmospheric CO_2.

5. Conclusions

- Lime–pozzolana mortars have been employed to cover the most representative surfaces of the Roman catacombs' walls. The observed mineralogical, chemical and textural properties of these mortars could provide an insight into the pasting techniques used by the ancient Roman builders inside the catacombs, where a specific microenvironment plays an important role in the chemical evolution of the mortar pastes.
- The measured environmental data inside the Saint Callistus and Domitilla catacombs show a constant temperature of 15–17 °C, a high CO_2 content (1700 to 3500 ppm) and a relative humidity close to 100%. These conditions and particularly the high CO_2 concentration speed-up the lime calcitization roughly by 500%.
- Roman builders made one to three mortar beds, using local aggregates. However, the in situ volcanic aggregate was not used. The high proportion in clay of the in situ tephra probably leads them to choose different sources of less altered aggregates. Hardened lime lumps inside the binder denote low water–mortar ratios for slaking.
- Frequently, a thin layer of pure lime was smeared onto the soft and crumbly natural surface of the host rock. Builders waited for the desiccation of this first bed to plaster a second bed of pure lime mortar. Two explanations are suggested: (i) providing hardening of this soft substrate and (ii) possible experiments to see how fast the lime cures in situ, given the specific atmosphere inside the catacomb.
- The aggregate–lime mixture shows a higher content of binder in comparison to contemporary written reports and other Roman monuments. The structure of these mortars shows (i) coarser aggregates and thicker beds on the inside; (ii) thin, smoothed, light and fine-grained external surfaces with low content of aggregates; and (iii) paintings and frescoes on the outside. The observed high porosity of the mortars can be attributed to cracking after drying linked with the high binder content.
- The high content in volcanic glass and unstable minerals in the aggregate helps the chemical reactions around the aggregate grains. Conversely, the fast calcitization under the hypogeal level of CO_2 and the porosity provide a ceiling to the cationic diffusion forming hydrous calcium aluminosilicates.
- This type of study is essential in the description of useful parameters and details on Roman mortars, thereby facilitating restoration. The final objective must be the use of materials and recipes compatible to the original mortar. We conclude that special restoration mortars must be used in those cases, where the original material is located in hypogeal environments.

Acknowledgements

We are very grateful to Rafael González, Maribel Ruiz and Marisa Vallejo of the Department of Geology, Museo Nacional de Ciencias Naturales (CSIC), Madrid, and to Olga Cazalla of the Universidad de Granada. Special thanks also to Ugo and Giusepe in the Roman catacombs. This research has been supported by the European Union Research Project CATS EVK4-CT200-00028 on biogenic decay prevention in Roman catacombs.

References

[1] M.L. Vitruvius, Los Diez Libros de Arquitectura. Ed. Iberia, Madrid, 2000.
[2] P. Degryse, J. Elsen, M. Waelkens, Study of ancient mortars from Sagalassos (Turkey) in view of their conservation, Cem. Concr. Res. 32 (2002) 1457–1463.
[3] A. Güleç, T. Tulun, Physico-chemical and petrographical studies of old mortars and plasters of Anatolia, Cem. Concr. Res. 27 (1997) 227–234.
[4] M.P. Riccardi, P. Duminuco, C. Tomasi, P. Ferloni, Thermal, microscopic and X-ray diffraction studies on some ancient mortars, Therm. Acta 321 (1998) 207–214.
[5] O. Cazalla, E. Sebastian, G. Cultrone, M. Nechar, M.G. Bagur, Three-way ANOVA interaction analysis and ultrasonic testing to evaluate air lime mortars used in cultural heritage conservation projects, Cem. Concr. Res. 29 (1999) 1749–1752.
[6] J. Garcia-Guinea, R. Abella, S. Sánchez-Moral, R. Benito, J.D. Martín-Ramos, Examining hydrated minerals using optically stimulated X-Ray diffraction, an inexpensive modification of traditional diffractometers, J. Sediment. Res. 70 (2000) 964–967.
[7] J. Garcia-Guinea, R. Ortiz, V. Correcher, A. LaIglesia, J.D. Martín-Ramos, Improvements to X-ray diffractometer: heaters, hygrometry, thermo-differential and spectra analyses, Rev. Sci. Instrum. 72 (2001) 4005–4007.
[8] H.W. Nesbitt, G.M. Young, Formation and diagénesis of weathering profiles, J. Geol. 97 (1989) 129–147.
[9] H.W. Nesbitt, R.E. Wilson, Recent chemical weathering of basalts, Am. J. Sci. 292 (1992) 740–777.
[10] D. Langmuir, Aqueous Environmental Geochemistry, Prentice-Hall, New Jersey, 1997, 600 pp.
[11] L.N. Plummer, D.L. Parkhurst, T.M.L. Wigley, Critical review of the kinetics of calcite dissolution and precipitation, in: E.A. Jenne (Ed.), Chemical Modelling of Aqueous Systems, Am. Chem. Soc. Symp. Ser., vol. 93, Am. Chem. Soc, Washington, DC, 1979, pp. 537–573.
[12] E. Busenberg, L.N. Plummer, A comparative study of the dissolution and crystal growth kinetics of calcite and aragonite, in: F.A. Mumpton

(Ed.), Studies in Diagenesis, U.S. Geological Survey Bulletin, vol. 1578, 1986, pp. 139–168.
[13] L.N. Plummer, D.L. Parkhurst, G.W. Fleming, S.A. Dunkle, PHRQPITZ a computer program incorporating Pitzer's equations for calculation of geochemical reactions in brines, U.S. Geological Survey Water Resources Investigation Report, vol. 88, U.S. Government Printing Office, Washington, DC, 1988, p. 4153.
[14] D.K. Nordstrom, L.N. Plummer, D. Langmuir, E. Busenberg, H.M. May, Revised chemical equilibrium data for major water–mineral reactions and their limations, in: E.A. Jenne (Ed.), Chemical Modeling of Aqueous Systems, Am. Chem. Soc. Symp. Ser., vol. 93, Am. Chem. Soc, Washington, DC, 1990, pp. 857–892.
[15] J.P. Adam, in: Batsford (Ed.), Roman Building: Materials and Techniques, 1994, 360 pp.
[16] R. Hayen, K. Van Balen, D. Van Gemert, The influence of production processes and mortar compositions on the properties of historical mortars, 9th Canadian Masonry Symposium, Publ. Inst. For Research in Construction, Univ. New Brunswick, Canada, 2001, 12 pp.
[17] G. Baronio, L. Binda, N. Lombardini, The role of brick pebbles and dust in conglomerates based on hydrated lime and crushed bricks, Constr. Build. Mater. 11 (1997) 33–40.
[18] G. Giaccio, R. Zerbino, Failure mechanism of concrete. Combined effects of coarse aggregates and strength level, Adv. Cem. Based Mater. 7 (1998) 41–416.
[19] A.H.P. Maurenbrecher, M.Z. Rousseau, Review of factors affecting the durability of repointing mortars for older masonry, 9th Canadian Masonry Symposium, Publ. Inst. For Research in Construction, Univ. New Brunswick, Canada, 2001, 12 pp.
[20] M.A. Plinius, Historia Natural, Facsimile, ITGE, 1998, (1629) 2 vols.
[21] S. Lodola, Studio archeometrico di laterizi e malte dallo scavo archeologico di Villa maria (Lomello, pavia). Thesis for the Degree in Geology, (1993) University of Pavia: 118.
[22] J.P. Ollivier, J.C. Maso, B. Bourdette, Interfacial transition zone in concrete, Adv. Cem. Based Mater. 2 (2) (1995) 30–38.
[23] L.N. Plummer, T.M.L. Wigley, D.L. Parkhurst, The kinetics of calcite dissolution in CO_2–water systems at 5 to 6 °C and 0.0 to 1.0 atm CO_2, Am. J. Sci. 278 (1978) 179–216.